Supplementary Material

T-Nb_2O_5 embedded carbon nanosheet with superior reversibility and rate capability as an anode for high energy Li-ion capacitors

Dong Li,[‡a] Jing Shi,*[a] Haolin Liu,[a] Chunyue Liu,[a] Guanghe Dong,[a] Hao Zhang,[a] Yunpeng Yang,[a] Gaofei Lu,[a] Huanlei Wang*[a]

[a] *School of Materials Science and Engineering, Ocean University of China, Qingdao 266100, People's Republic of China*

‡ These authors contribute equally to this work.

* Corresponding author.

E-mail address: shijing@ouc.edu.cn (J. Shi); huanleiwang@gmail.com (H. Wang).

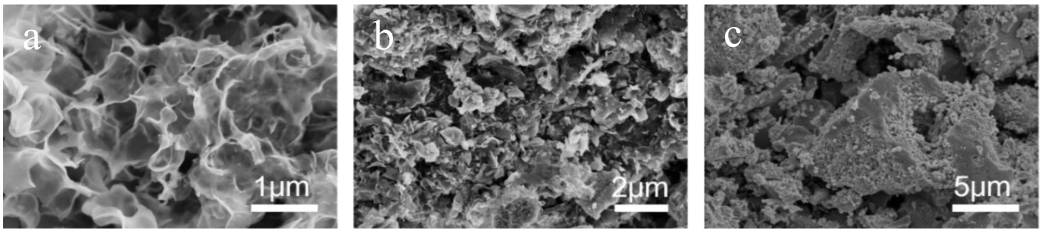

Fig. S1 (a) SEM image of GCN. (b) SEM image of *T*-Nb_2O_5/GCN. (c) SEM image of *T*-Nb_2O_5.

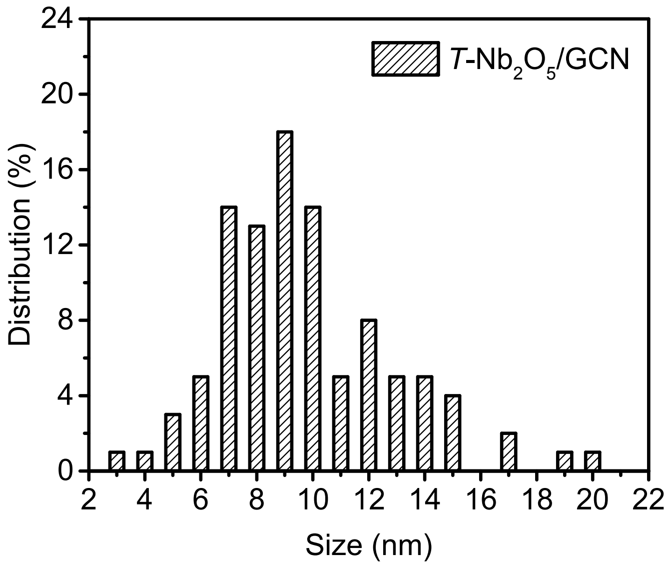

Fig. S2 The Nb_2O_5 particle size distribution of *T*-Nb_2O_5/GCN, which is based on the measurement of 100 particles in their maximum dimension.

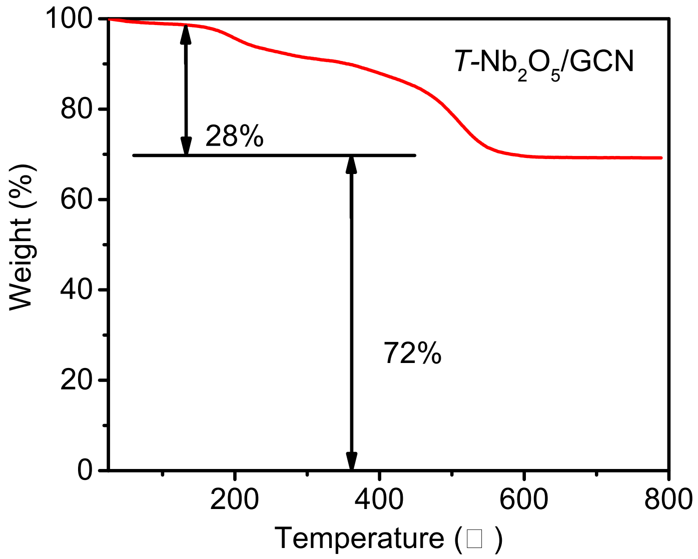

Fig. S3 TG analysis of *T*-Nb_2O_5/GCN composite in air flow.

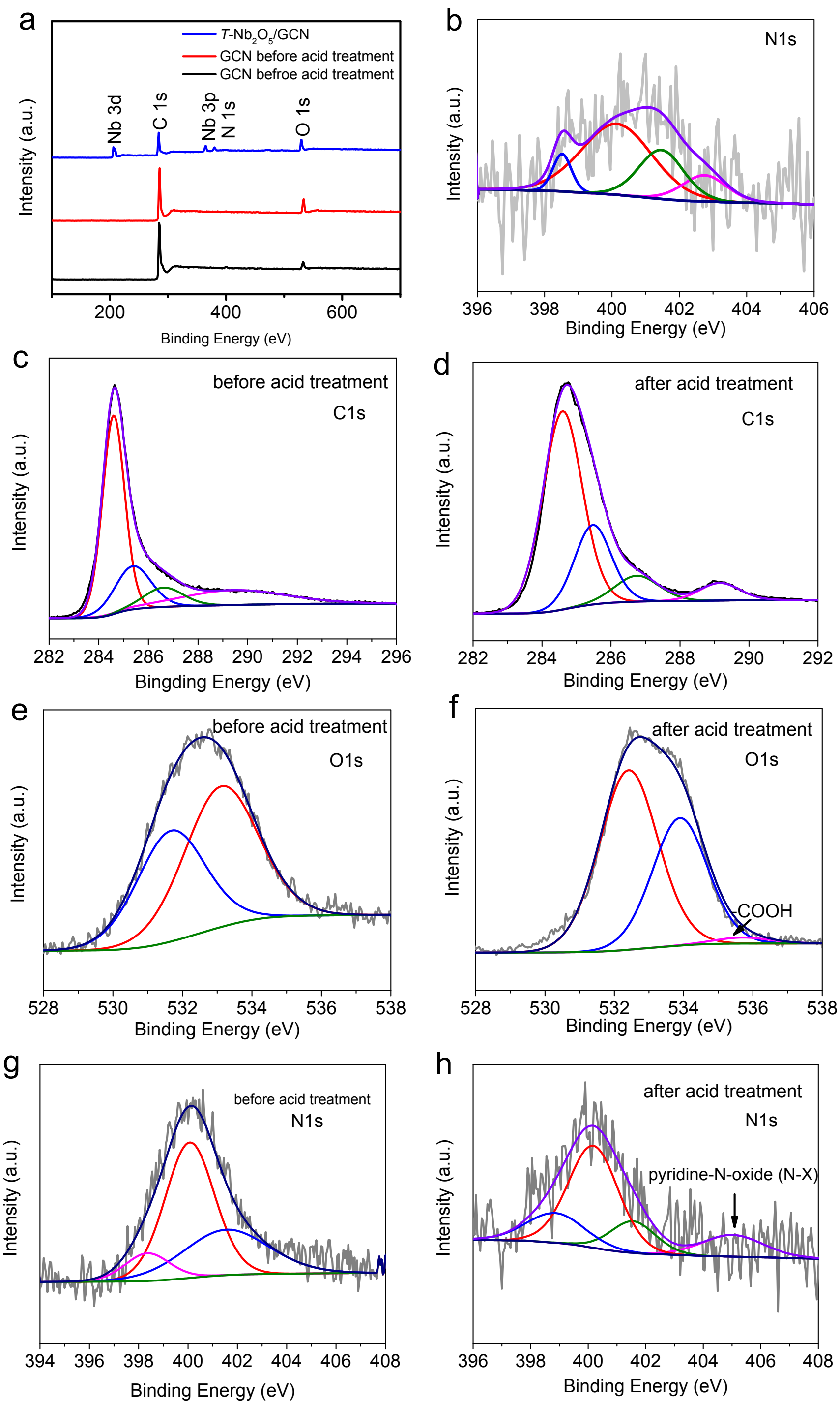

Fig. S4 (a) The survey spectra. (b) N 1s XPS spectra of *T*-Nb_2O_5/GCN. (c) C 1s XPS spectra of GCN before acid treatment. (d) C 1s XPS spectra of GCN after acid treatment. (e) O 1s spectra of GCN before acid treatment. (f) O 1s XPS spectra of GCN after acid treatment. (g) N 1s spectra of GCN before acid treatment. (h) N 1s XPS spectra of GCN after acid treatment.

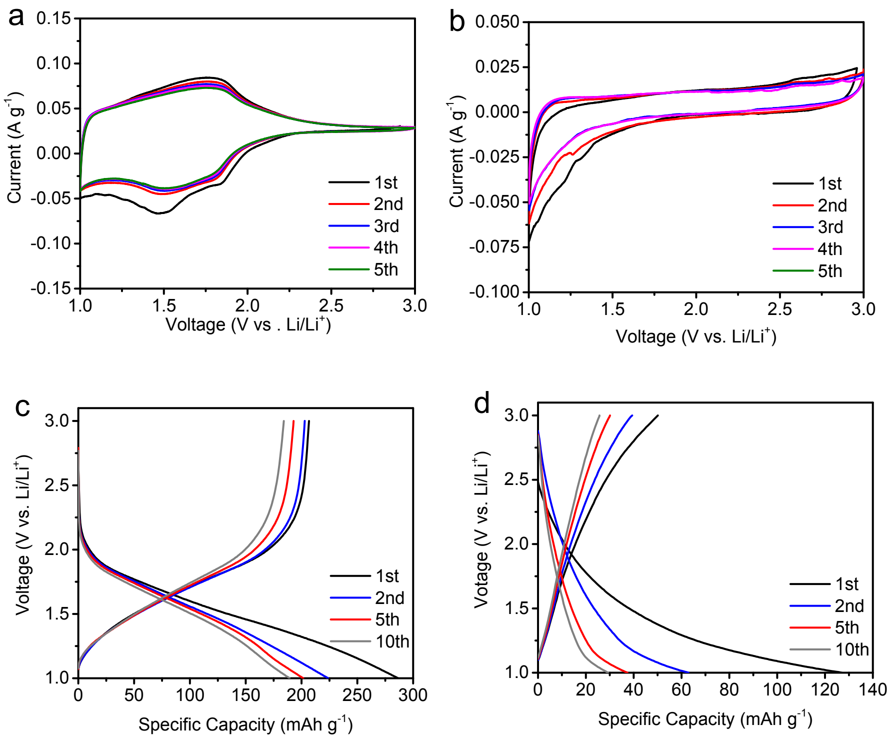

Fig. S5 (a) CV curves of *T*-Nb_2O_5 at 0.1 mV s^{-1}. (b) CV curves of GCN at 0.1 mV s^{-1}. (c)

Galvanostaic charge-discharge profiles of T-Nb_2O_5 at 0.1 A g^{-1}. (d) Galvanostaic charge-discharge profiles of GCN at 0.1 A g^{-1}.

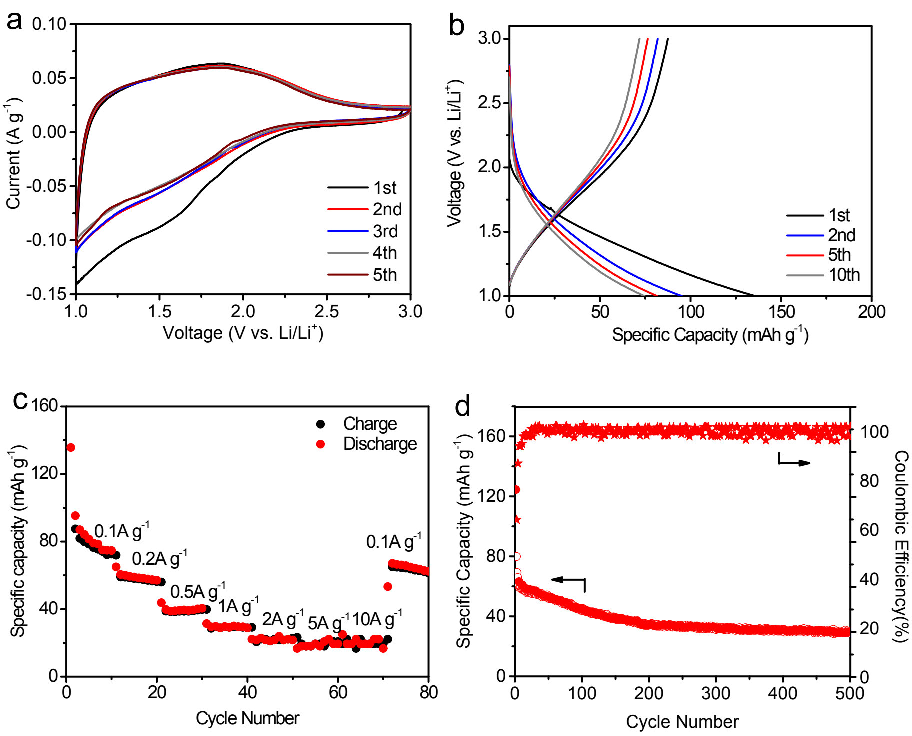

Fig. S6 (a) CV curves of T-Nb_2O_5/GCN (50%) at 0.1 mV s^{-1}. (b) Galvanostaic charge-discharge profiles of T-Nb_2O_5/GCN (50%) at 0.1 A g^{-1}. (c) Rate capacities at various current densities from 0.1 to 10 A g^{-1}. (d) Cycling performance and the related coulombic efficiency for T-Nb_2O_5/GCN (50%) at 2 A g^{-1} for 500 cycles.

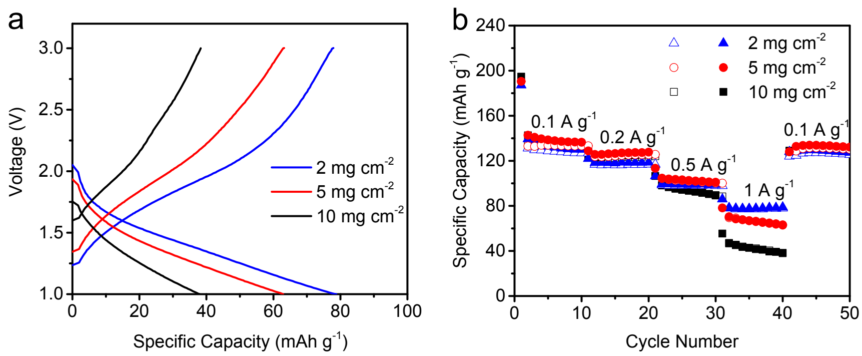

Fig. S7 (a) Galvanostatic charge-discharge curves for *T*-Nb_2O_5/GCN electrode. (b) The *T*-Nb_2O_5/GCN electrode at a current density of 1 A g^{-1} for the mass loadings of 2, 5, and 10 mg cm^{-2}.

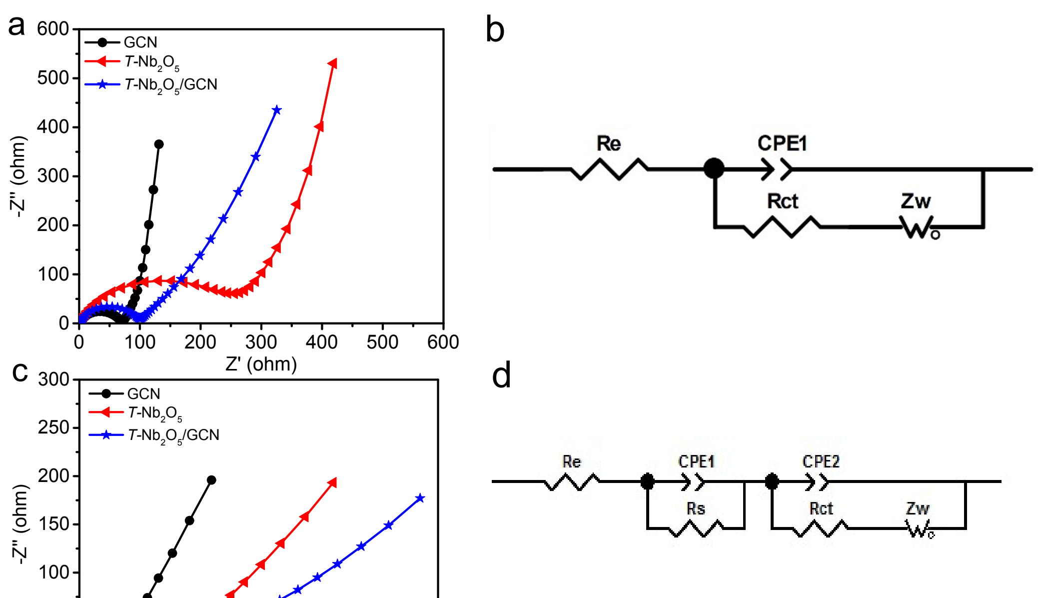

Fig. S8 Nyquist plots of GCN, *T*-Nb_2O_5 and *T*-Nb_2O_5/GCN electrodes (a) before cycling and (c) after 500 cycles. The used equivalent circuits for Nyquist plot simulation: (b) before cycling and (d) after 500 cycles.

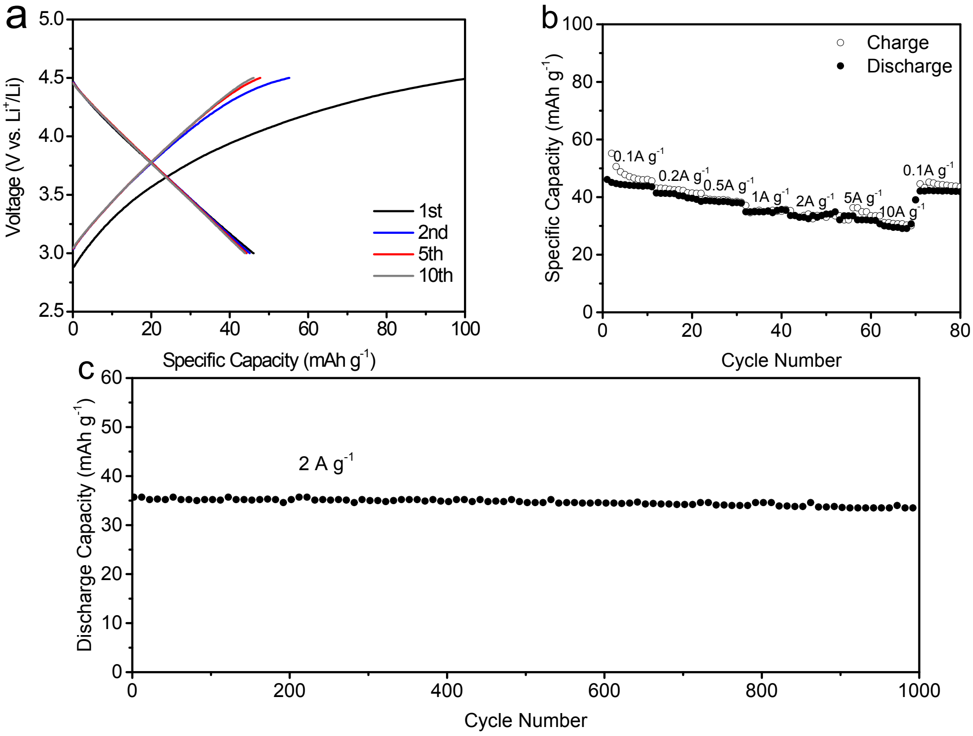
a
b
c
Voltage (V vs. Li+/Li)
Specific Capacity (mAh g-1)
1st
2nd
5th
10th
Specific Capacity (mAh g-1)
Cycle Number
Charge
Discharge
0.1A g-1
0.2A g-1
0.5A g-1
1A g-1
2A g-1
5A g-1
10A g-1
0.1A g-1
Discharge Capacity (mAh g-1)
2 A g-1
Cycle Number

Fig. S9 (a) Typical charge and discharge curves of GCN cathode at 0.1 A g^{-1}; (b) Rate capability of GCN at various current densities; (c) Cycling performance of the GCN cathode at 2 A g^{-1}.

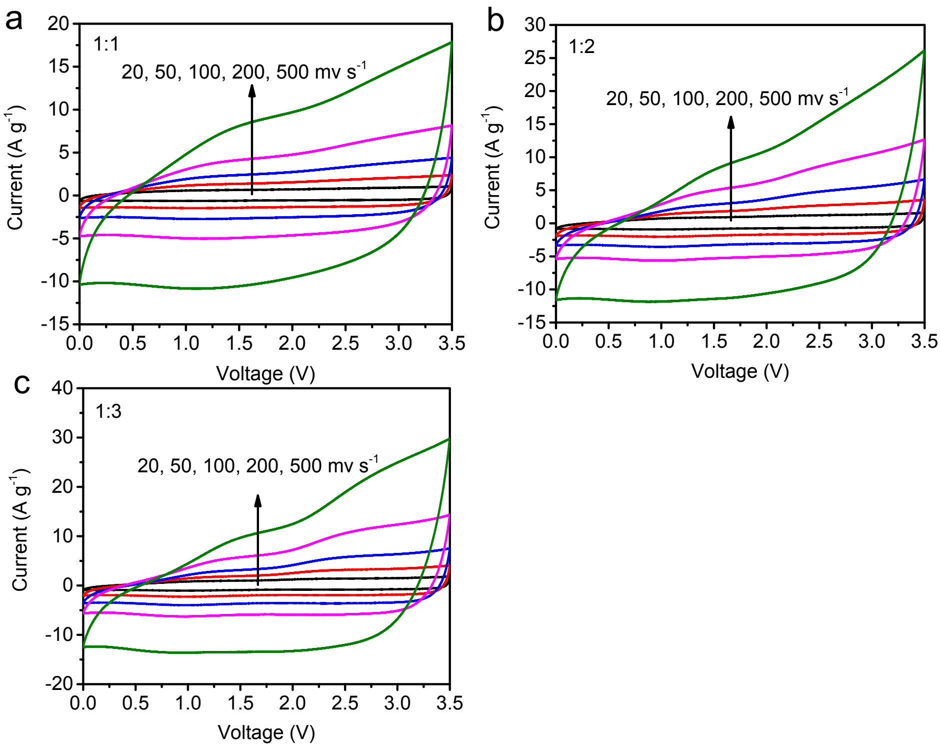

Fig. S10 CV curves of Li-ion capacitors at various sweep rates with different anode to cathode mass ratios of (a) 1:1, (b) 1:2, (c) 1:3.

Table S1 Comparison with the performance of previously reported Li-ion capacitors.

Hybrid system	Voltage Window	Energy Density/ Power Density	Cyclability	Ref.
Nb_2O_5//GCN (Li^+)	0-3.5 V	129 Wh kg^{-1} at 145.29 W kg^{-1} 50.6 Wh kg^{-1} at 16703.75 W kg^{-1}	80% after 10000 cycles at 5A g^{-1}	This work
CNT/Nb_2O_5//AC (Li^+)	0.5-3 V	33.5Wh kg^{-1} at 83 W kg^{-1} ~4 Wh kg^{-1} at 4000 W kg^{-1}	–	1
TiO_2//CNT-AC (Li^+)	1-3 V	59.6 Wh kg^{-1} at 120 W kg^{-1} 31.2 Wh kg^{-1} at 7000 W kg^{-1}	–	2
PF16//FRGO (Li^+)	0-4.2 V	148.3 Wh kg^{-1} at 141W kg^{-1} 71.5 Wh kg^{-1} at 7800W kg^{-1}	68% after 2000 cycles at 1.86A g^{-1}	3
Nb_2O_5//AC (Li^+)	1-3.5 V	95.55 Wh kg^{-1} at 191 W kg^{-1} 65/39 Wh kg^{-1}at 5350.9 W kg^{-1}	–	4
CNT_S-Nb_2O_5//AC (Li^+)	0.5-3 V	~50 Wh kg^{-1} at 86.46 W kg^{-1} 14.77 Wh kg^{-1} at 6753.5 W kg^{-1}	–	5
$_P$-NbN//APDC (Li^+)	0-4 V	149 Wh kg^{-1} at 200 W kg^{-1} 5 Wh kg^{-1} at 45000 W kg^{-1}	~95% after 15000 cycles at 1 A g^{-1}	6
Ni-Co LDH/3D RGO NF//AC (Li^+)	0-1.6 V	38.6 Wh kg^{-1} at 69.48 W kg^{-1} 3.65 W h kg^{-1}at 7231.6 W kg^{-1}	70% after 4000 cycles at 10 mA cm^{-2}	7
SnO_2–C//MC (Li^+)	0-4 V	110 Wh kg^{-1} at 90 W kg^{-1} 45 Wh kg^{-1} at 2960 W kg^{-1}	80% after 2000 cycles at 1 A g^{-1}	8
AC//Li_2CoPo_4F (Li^+)	0-3 V	47 Wh kg^{-1} at 215 W kg^{-1} 24 Wh kg^{-1} at 1607 W kg^{-1}	92% after 30000 cycles at 1.1A g^{-1}	9
T-Nb_2O_5 /graphene//MC (Li^+)	0.8-3 V	48 Wh kg^{-1} at 690 W kg^{-1} 13 Wh kg^{-1} at 16000 W kg^{-1}	~92% after 3000 cycles at 1A g^{-1}	10

Graphene wrapped LTO//AC (Li^+)	1-2.5 V	50 Wh kg^{-1} at ~15 W kg^{-1} 15 Wh kg^{-1} at 2500 W kg^{-1}	75% after 1000 cycles at 1mA cm^{-2}	11
$H_2Ti_{11.85}Nb_{0.15}O_{25}$//AC ($Li^+$)	0-2.8 V	24.3Wh kg^{-1} at1794.6 W kg^{-1} 11.3Wh kg^{-1} at 5821.3W kg^{-1}	84% after 10000 cycles at 3A g^{-1}	12
MnO/C//CNS (Li^+)	1-4 V	100 Wh kg^{-1} at 83 W kg^{-1} 30 Wh kg^{-1} at 20000 W kg^{-1}	70% after 5000 cycles at 5A g^{-1}	13
S-ATNT//OMC (Li^+)	0-3 V	25 Wh kg^{-1} at 3000 W kg^{-1} 42 Wh kg^{-1} at <300 W kg^{-1}	–	14
MnO-C//AC (Li^+)	0-4 V	227 Wh kg^{-1} at ~60 W kg^{-1} ~20 Wh kg^{-1} at 2952 W kg^{-1}	92.5% after 3500 cycles at 4 A g^{-1}	15
GDY//AC (Li^+)	2-4 V	112.2 Wh kg^{-1} at 400.1 W kg^{-1} 95.1 Wh kg^{-1} at 1000.4 W kg^{-1}	94.7% after 1000 cycles at 0.2A g^{-1}	16
TNO@C//CF_S (Li^+)	0.8-3.2V	110.4 Wh kg^{-1} at99.58 W kg^{-1} 20 Wh kg^{-1} at 5464 W kg^{-1}	77% after 1500 cycles at 0.2A g^{-1}	17
Si/FG/C//CPAC (Li^+)	2-4.5V	159 Wh kg^{-1} at 945 W kg^{-1} 99 Wh kg^{-1} at 31235 W kg^{-1}	80% after 1000 cycles at 1A g^{-1}	18
Ti3C_2Tx/CNTs//AC (Li^+)	1-4 V	67 Wh kg^{-1} at 258 W kg^{-1} 19 Wh kg^{-1} at 5297 W kg^{-1}	81.3% after 5000 cycles at 2A g^{-1}	19
m-Nb_2O_5-C//MSP-20 (Li^+)	0-3 V	20 Wh kg^{-1} at 12137 W kg^{-1} 15 Wh kg^{-1} at 18510 W kg^{-1}	90% after 1000 cycles at 1A g^{-1}	20
T-Nb_2O_5@C//MSP-20 (Li^+)	1-3.5 V	63 Wh kg^{-1} at 70 W kg^{-1} 5 Wh kg^{-1} at 16528 W kg^{-1}	~80% after 1000 cycles at 1A g^{-1}	21
LTP//AC (Li^+)	0-3 V	14 Wh kg^{-1} at 45 W kg^{-1} 0.8 Wh kg^{-1} at 180 W kg^{-1}	–	22

PANI//LMB-NB (Li^+)	0-3 V	42 Wh kg^{-1} at1500 W kg^{-1} 15 Wh kg^{-1} at5350 W kg^{-1}	94% after 30000 cycles at 2.25A g^{-1}	23
Graphite//AC (Li^+)	1.5-4.5V	103.8 Wh kg^{-1} at ~65 W kg^{-1}	85% after 10000 cycles at 0.12A g^{-1}	24
$H_2Ti_6O_3$//CMK-3 (Li^+)	1-3.5 V	90 Wh kg^{-1} at ~600 W kg^{-1}	80% after 1000 cycles at 0.15A g^{-1}	25
$LiCrTiO_4$//AC (Li^+)	1-3V	23 Wh kg^{-1} at 800 W kg^{-1} ~4.5Wh kg^{-1} at ~4000 W kg^{-1}	~100% after 1000 cycles at 2A g^{-1}	26

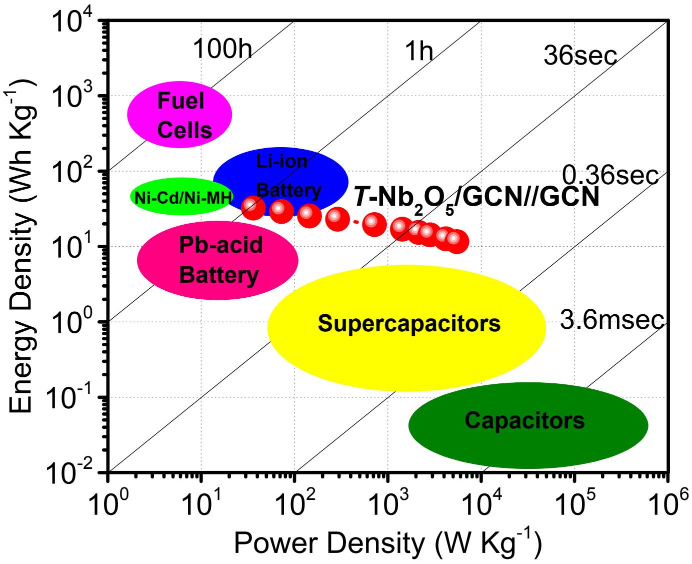

Fig. S11 Ragone plot of *T*-Nb_2O_5/GCN//GCN Lithium ion capacitors in comparison with other commercial energy storage devices.

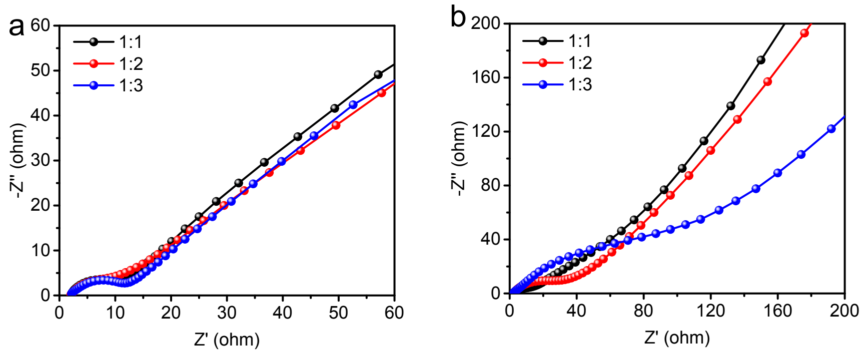

Fig. S12 Electrochemical impendence spectra of LICs with various anode to cathode mass ratios of 1:1, 1:2 and 1:3, (a) before cycling and (b) after 10000 cycles.

Note and references

1 X. Wang, G. Li, Z. Chen, V. Augustyn, X. Ma, G. Wang, B. Dunn, Y. Lu, *Adv. Energy Mater.*, 2011, **1**, 1089-1093.

2 Z. Chen, Y. Yuan, H. Zhou, X. Wang, Z. Gan, F. Wang, Y. Lu, *Adv. Mater.*, 2014, **26**, 339-345.

3 T. Zhang, F. Zhang, L. Zhang, Y. Lu, Y. Zhang, X. Yang, Y. Ma, Y. Huang, *Carbon*, 2015, **92**, 106-118.

4 B. Deng, T. Lei, W. Zhu, L. Xiao, J. Liu, *Adv. Funct. Mater.*, 2018, **28**, 1704330.

5 X. Wang, G. Li, R. Tjandra, X. Fan, X. Xiao, A. Yu, *RSC Adv.*, 2015, **5**, 41179-41185.

6 P. Wang, R. Wang, J. Lang, X. Zhang, Z. Chen, X. Yan, *J. Mater. Chem. A*, 2016, **4**, 9760-9766.

7 X. Bai, Q. Liu, H. Zhang, J. Liu, Z. Li, X. Jing, Y. Yuan, L. Liu, J. Wang, *Electrochim. Acta*, 2016, **215**, 492-499.

8 W.-H. Qu, F. Han, A.-H. Lu, C. Xing, M. Qiao, W.-C. Li, *J. Mater. Chem. A*, 2014, **2**, 6549.

9 K. Karthikeyan, S. Amaresh, K.J. Kim, S.H. Kim, K.Y. Chung, B.W. Cho, Y.S. Lee, *Nanoscale*, 2013, **5**, 5958-5964.

10 L. Kong, C. Zhang, S. Zhang, J. Wang, R. Cai, C. Lv, W. Qiao, L. Ling, D. Long, *J. Mater. Chem. A*, 2014, **2**, 17962-17970.

11 H. Kim, K.-Y. Park, M.-Y. Cho, M.-H. Kim, J. Hong, S.-K. Jung, K.C. Roh, K. Kang, *ChemElectroChem*, 2014, **1**, 125-130.

12 J.H. Lee, H.-K. Kim, E. Baek, M. Pecht, S.-H. Lee, Y.-H. Lee, *J. Power Sources*, 2016, **301**, 348-354.

13 Y. Zhao, Y. Cui, J. Shi, W. Liu, Z. Shi, S. Chen, X. Wang, H. Wang, *J. Mater. Chem. A*, 2017, **5**, 15243-15252.

14 D.-W. Wang, H.-T. Fang, F. Li, Z.-G. Chen, Q.-S. Zhong, G.Q. Lu, H.-M. Cheng, *Adv. Funct. Mater.*, 2008, **18**, 3787-3793.

15 C. Liu, C. Zhang, H. Song, C. Zhang, Y. Liu, X. Nan, G. Cao, *Nano Energy*, 2016, **22**, 290-300.

16 H. Du, H. Yang, C. Huang, J. He, H. Liu, Y. Li, *Nano Energy*, 2016, **22**, 615-622.

17 X. Wang, G. Shen, *Nano Energy*, 2015, **15**, 104-115.

18 Q. Lu, B. Lu, M. Chen, X. Wang, T. Xing, M. Liu, X. Wang, *J. Power Sources*, 2018, 398, 128-136.

19 P. Yu, G. Cao, S. Yi, X. Zhang, C. Li, X. Sun, K. Wang, Y. Ma, *Nanoscale*, 2018, **10**, 5906-5913.

20 E. Lim, H. Kim, C. Jo, J. Chun, K. Ku, S. Kim, H.I. Lee, I.S. Nam, S. Yoon, K. Kang, J. Lee, *ACS Nano*, 2014, **8**, 8968-8978.

21 E. Lim, C. Jo, H. Kim, M.H. Kim, Y. Mun, J. Chun, Y. Ye, J. Hwang, K.S. Ha, K.C. Roh, K. Kang, S. Yun, J. Lee, *ACS Nano*, 2015, **9**, 7497-7505.

22 V. Aravindan, W. Chuiling, M.V. Reddy, G.V. Rao, B.V. Chowdari, S. Madhavi, *Phys. Chem. Chem. Phys.*, 2012, **14**, 5808-5814.

23 K. Kaliyappan, S. Amaresh, Y.S. Lee, ACS Appl. Mater. Interfaces, 2014, **6**, 11357-11367.

24 V. Khomenko, E. Raymundo-Piñero, F. Béguin, *J. Power Sources*, 2008, **177**, 643-651.

25 Y. Wang, Z. Hong, M. Wei, Y. Xia, *Adv. Funct. Mater.*, 2012, **22**, 5185-5193.

26 V. Aravindan, W. Chuiling, S. Madhavi, *J. Mater. Chem.*, 2012, **22**, 16026.